UC Irvine
UC Irvine Previously Published Works

Title

The membrane protein MiRP3 regulates Kv4.2 channels in a KChIP-dependent manner

Permalink

Journal

The Journal of Physiology, 588(14)

ISSN

Authors

Levy, Daniel I
Cepaitis, Egle
Wanderling, Sherry
et al.

Publication Date

2010-07-15

DOI

Copyright Information

Peer reviewed

The membrane protein MiRP3 regulates Kv4.2 channels in a KChIP-dependent manner

Daniel I. Levy[1,2], Egle Cepaitis[1], Sherry Wanderling[1], Peter T. Toth[1], Stephen L. Archer[1] and Steve A. N. Goldstein[2]

[1]*Departments of Medicine and* [2]*Pediatrics and the Institute for Molecular Pediatric Sciences, Biological Sciences Division, Pritzker School of Medicine, University of Chicago, Chicago, IL 60637, USA*

MiRP3, the single-span membrane protein encoded by *KCNE4*, is localized by immunofluorescence microscopy to the transverse tubules of murine cardiac myocytes. MiRP3 is found to co-localize with Kv4.2 subunits that contribute to cardiac transient outward potassium currents (I_{to}). Whole-cell, voltage-clamp recordings of human MiRP3 and Kv4.2 expressed in a clonal cell line (tsA201) reveal MiRP3 to modulate Kv4.2 current activation, inactivation and recovery from inactivation. MiRP3 shifts the half-maximal voltage for activation ($V_{1/2}$) ∼20 mV and slows time to peak ∼100%. In addition, MiRP3 slows inactivation ∼100%, speeds recovery from inactivation ∼30%, and enhances restored currents so they 'overshoot' baseline levels. The cytoplasmic accessory subunit KChIP2 also assembles with Kv4.2 in tsA201 cells to increase peak current, shift $V_{1/2}$ ∼5 mV, slow time to peak ∼10%, slow inactivation ∼100%, and speed recovery from inactivation ∼250% without overshoot. Simultaneous expression of all three subunits yields a biophysical profile unlike either accessory subunit alone, abolishes MiRP3-induced overshoot, and allows biochemical isolation of the ternary complex. Thus, regional heterogeneity in cardiac expression of MiRP3, Kv4.2 and KChIP2 in health and disease may establish the local attributes and magnitude of cardiac I_{to}.

Introduction

MinK-related peptides (MiRPs) are single-span membrane proteins that assemble with voltage-gated K$^+$ channels to establish channel behaviour in native cells (Abbott & Goldstein, 1998; McCrossan & Abbott, 2004). Although the *KCNE4* gene encoding MiRP subtype 3 (MiRP3) is widely expressed (Grunnet *et al.* 2002), the roles of MiRP3 in natural physiology remain poorly understood. Levels of the *KCNE4* transcript in human cardiac ventricle are robust and increase in patients with congestive failure (Bendahhou *et al.* 2005; Lundquist *et al.* 2005; Radicke *et al.* 2006), suggesting a regulatory function for MiRP3 in the heart.

In experimental settings, MiRP3 inhibits the activity of KCNQ1 channel subunits. Coexpression with MiRP3 markedly reduces KCNQ1 currents in heterologous cells by direct subunit–subunit interactions via an as-yet unidentified mechanism (Grunnet *et al.* 2002; Manderfield *et al.* 2009; Vanoye *et al.* 2009). Likewise, transient expression of MiRP3 in Chinese hamster ovary (CHO) cells suppresses current resulting from stable expression of KCNQ1 with MinK (Lundquist *et al.* 2005), the two subunits that produce the slow cardiac delayed rectifier current I_{Ks} (Barhanin *et al.* 1996; Sanguinetti *et al.* 1996; Splawski *et al.* 1997; Sesti & Goldstein, 1998). The observation that MiRP3 forms a ternary complex with KCNQ1 and MinK in CHO cells suggests it may down-regulate native I_{Ks} currents (Manderfield & George, 2008).

In a species-dependent manner, Kv4.3 or Kv4.2 produce cardiac $I_{to,fast}$ (Rosati *et al.* 2001; Patel *et al.* 2002; Guo *et al.* 2005; Niwa *et al.* 2008) channels by assembly with KChIP2 cytoplasmic accessory subunits (An *et al.* 2000; Kuo *et al.* 2001); a subpopulation of myocytes employ Kv1.4 to create $I_{to,slow}$ channels (Guo *et al.* 1999; Niwa & Nerbonne, 2010). Hereafter in this report, I_{to} refers solely to $I_{to,fast}$. Both Kv4.3/Kv4.2 and KChIP2 show heterogeneity in protein and transcript levels across the healthy ventricular wall (Patel & Campbell, 2005) and KChIP2 transcription is reduced in human heart failure (Radicke *et al.* 2006). Homologues of MiRP3 and Kv4.2 are found to interact in chemosensory and mechanosensory neurons of the nematode *C. elegans* (Bianchi *et al.* 2003). Further,

expression of MiRP3 with Kv4.3 and KChIP2 in CHO cells is reported to alter channel function (Radicke *et al.* 2006).

Based on the high levels of *KCNE4* mRNA in myocardium and functional effects of MiRP3 on Kv4.3 with KChIP2 in tissue culture cells, we sought further evidence for modulation of cardiac I_{to} by MiRP3. Here, MiRP3 and Kv4.2 are found to co-localize to the transverse tubules (T-tubules) of rat cardiac myocytes. In tsA201 cells, voltage-clamp studies demonstrate that MiRP3 slows Kv4.2 activation and inactivation and induces larger than baseline currents on recovery from inactivation (overshoot), effects that are different from those of KChIP2 alone. Expression of Kv4.2, KChIP2 and MiRP3 in tissue culture cells reveals formation of a ternary complex by co-immunoprecipitation and biophysical parameters under voltage-clamp that cannot accrue from mixtures of Kv4.2–KChIP2 and Kv4.2–MiRP3 channels. We therefore support the hypothesis of Radicke *et al.* (2006) that native cardiac I_{to} operates in a manner that reflects the balance of local expression of these proteins.

Methods

Molecular biology

Human coding sequences for MiRP3 (*KCNE4*; NM_080671), Kv4.2 (*KCND2*; NM_012281) and KChIP2.1 (*KCNIP2*, variant 3; NM_173192) were subcloned with a Kozak consensus sequence (GCCACC) before the initiating methionine into the pRAT vector, which is optimized for both oocyte and mammalian expression (Bockenhauer *et al.* 2001). An epitope-tagged variant of Kv4.2 (Kv4.2–1d4) was engineered by introducing a linker (RVPDGDPD) followed by the bacterial rhodopsin sequence, 1d4 (ETSQVAPA), at the carboxy terminus. The interacting sequence of filamin A was similarly subcloned into pRAT with the 1d4 epitope tag (fil–1d4). For co-transfection of Kv4.2 and KChIP2 into tsA201, a pIRES vector was used containing KChIP2 in the 5′ multiple cloning site (MCS) and Kv4.2 in the 3′ MCS.

Antibodies

Generation of rabbit polyclonal antibodies to human MiRP3 residues 136–150 (for immunofluorescence studies) and 151–170 (for biochemistry) has been described previously (Levy *et al.* 2008). The MiRP3$_{136-150}$ antibody was directly conjugated with the Alexa Fluor 594 carboxylic, succinimidyl ester reagent (Invitrogen, Carlsbad, CA, USA) using the protocol supplied by the company. Anti-Kv4 antibodies were similarly raised and affinity purified, using the peptide sequence CLEKTTNHEFVDEQVFEES, first described by Yao *et al.* (1999). Goat polyclonal antibody to MiRP3 was purchased

from Santa Cruz Biotechnology (N-14; Santa Cruz, CA, USA). Rabbit polyclonal antibody to Kv4.2 for confirmatory immunofluorescence studies was purchased from Chemicon/Millipore (AB5360; Temecula, CA, USA). Mouse monoclonal antibodies were purchased for KChIP2 (K60/73; UC Davis/NINDS/NIMH NeuroMab Facility, Davis, CA, USA) and the 1d4 epitope (National Cell Culture Center, Minneapolis, MN, USA).

Immunofluorescence

The animal experimentation was conducted in accordance with the *Guide for Care and Use of Laboratory Animals* (National Institutes of Health, Bethesda, MD, USA) and was approved by the local Institutional Animal Care and Use Committees. Following a lethal dose of pentobarbital ($120 \, \text{mg kg}^{-1}$), the heart was removed from a Sprague–Dawley rat and snap-frozen for histological sectioning. Sections $7 \, \mu\text{m}$ thick were fixed with cold methanol, blocked in 5% chicken serum, and stained overnight at $4°\text{C}$ with a 1:100 dilution of rabbit anti-Kv4 antibody. An Alexa Fluor 488 chicken anti-rabbit secondary IgG was applied for 1 h at room temperature before a second overnight incubation with a 1:100 dilution of rabbit anti-MiRP3$_{136-150}$ directly conjugated to Alexa Fluor 594. Samples were mounted with ProLong Gold antifade reagent containing 4′,6-diamidino-2-phenylindole (DAPI; Invitrogen) and then imaged by confocal microscopy with an α Plan-Apochromat $100\times/1.46$ objective.

Cell culture and transfection

Renal fibroblast cells (COS-7) and a T antigen-transformed clone of human embryonic kidney-293 cells (tsA201) were cultured in DMEM supplemented with 10% fetal bovine serum or newborn bovine serum, respectively. Melanoma M2 and A7 cell lines (kindly provided by Dr Fumihiko Nakamura) were grown in MEM with 10 mM Hepes, 8% newborn bovine serum and 2% fetal bovine serum; the A7 cells were supplemented with $200 \, \mu\text{g ml}^{-1}$ of active G418. All media contained penicillin ($100 \, \text{u ml}^{-1}$) and streptomycin ($100 \, \mu\text{g ml}^{-1}$), and cells were held at $37°\text{C}$ in humidified air with 5% CO_2. For patch-clamp experiments, tsA201 cells were transfected with 3–6 μg of plasmid DNA (including $0.25 \, \mu\text{g}$ of pEGFP vector; Clontech, Palo Alto, CA, USA) in T-25 flasks, by adding $200 \, \mu$l of calcium–phosphate–DNA buffer (CalPhos; Clontech) to 1.8 ml of medium; transfected cells were rinsed and passaged 2 h later into 35 mm culture dishes containing glass coverslips. In these experiments, the molar ratio of transfected DNA for MiRP3:Kv4.2 was 4:1, and for MiRP3:Kv4.2:KChIP2 was 4:1:1. For biochemistry experiments, tsA201 cell

transfections were scaled up to accommodate 35–40 μg of plasmid DNA in 150 mm dishes. COS-7, M2 and A7 cells were transfected with 20–30 μg of plasmid DNA in 150 mm dishes by adding 2 μl Lipofectamine per 1 μg DNA in accordance with the manufacturer's protocol. Cells were rinsed with fresh medium after 2 h and harvested 12–36 h later. Media, sera, antibiotics and Lipofectamine 2000 were purchased from Invitrogen.

Patch-clamp experiments

Whole-cell recordings from tsA201 cells were made 16–36 h after transfection, using an Axopatch 200A amplifier (Axon Instruments) and CLAMPEX software. Transfected cells were identified as those with green fluorescence during brief illumination with a mercury lamp, and typically represented 25% of the total population of cells. Pipette solution contained (in mM): 120 KF, 10 Hepes, 11 EGTA (free acid), 2 $MgCl_2$, 1 $CaCl_2$; titrated to pH 7.20 with ~30 KOH. Bath solution contained 150 NaCl, 10 Hepes, 2 KCl, 1 $MgCl_2$, 1.5 $CaCl_2$; titrated to pH 7.40 with ~5 NaOH. Macroscopic recordings of 1–16 nA were made at room temperature with borosilicate electrodes of 2–4 MΩ resistance, using series resistance compensation >80% to maintain voltage error below 6 mV.

Activation and inactivation were analysed from currents recorded during a family of 500 ms voltage pulses between −80 and +80 mV that were delivered at 0.17 Hz from V_{hold} of −100 mV. Conductance was calculated by dividing peak currents as a function of driving force, determined by the Goldman–Hodgkin–Katz equation (Clay, 2000). Inactivation of Kv4.2 was fitted with either the single exponential function ($Ae^{-t/\tau} + C$), where t represents time (ms), τ represents the time constant of decay, A represents the inactivating component, and C is the residual component of non-inactivating current; or the dual-exponential function, ($A_f e^{-t/\tau f} + A_s e^{-t/\tau s} + C$), for which τ_f and τ_s represent the fast and slow time constants, and A_f and A_s reflect the weighted components of fast and slow decay, respectively. Comparison of the single-exponential to dual-exponential decay was made by modelling inactivation from the experimentally derived variables and comparing the time to reach 1/e of the peak current. The steady-state inactivation of Kv4.2 was examined from a holding potential of −100 mV with test pulses delivered at 0.2 Hz from −120 to 0 mV, held for 2.5 s followed by a brief pulse to +40 mV to measure current from non-inactivated channels. Recovery from inactivation was measured by a two-pulse protocol with a variable interpulse interval at −100 mV. The per cent recovery (R) was based on the difference between the first plateau current (C_1) and the second peak current (P_2), as compared to the inactivation that followed the first peak current (P_1): R = 100% * ($P_2 − C_1$)/($P_1 − C_1$).

Biochemistry

Pellets of harvested cells were solubilized for 45 min in lysis buffer containing (in mM): 100 NaCl, 40 KCl, 20 K-Hepes, 1 Na-EDTA, 10% v/v glycerol, 1% Triton X-100 (Roche Applied Science, Indianapolis, IN, USA) and protease-inhibitor tablets (Roche), pH 7.4. Insoluble material was removed by centrifugation. Immuno-purification of epitope-tagged proteins was performed as before by Kim *et al.* (2004*a*) with anti-1d4 monoclonal antibody (National Cell Culture Center, Minneapolis, MN, USA) linked to sepharose beads and elution with 1 mg ml^{-1} 1d4 peptide. MiRP3 purification was performed by overnight incubation with rabbit anti-MiRP3$_{151-170}$ followed by adsorption to protein A sepharose beads (Amersham Biosciences, Piscataway, NJ, USA) and elution with 1 mg ml^{-1} antigenic peptide. KChIP2 precipitation was similarly performed, except that elution used 4% SDS. Cell lysates and purified proteins were fractionated by SDS-PAGE and transferred to nitrocellulose membranes for Western blotting. Blots were imaged on a Licor Odyssey (Lincoln, NE, USA) using fluorescent secondary antibodies.

Yeast two-hybrid assay

A 348 bp sequence corresponding to the 116 cyto-plasmic residues of MiRP3 was inserted into a vector optimized for the yeast two-hybrid assay, pDBleu, in frame with the Gal4 binding domain. This bait plasmid was stably incorporated into yeast, which were then transformed with ~1 × 10^6 clones from a human heart library containing a transcriptional-activation domain (ProQuest library, Invitrogen) and screened for their ability to grow on His$^-$ medium. Strong interactors were validated by co-transformation into yeast with the original bait plasmid and screened by ability to grow on Ura$^-$ medium, 5-flouro-orotic acid sensitivity and β-Gal activity.

Results

Kv4.2 and MiRP3 co-localize to T-tubules of rat ventricle

Immunofluorescent labelling of MiRP3 and Kv4.2 was performed in left ventricle sections of rat heart, and confocal microscopy was used to reveal co-localization of both proteins to the transverse tubules (Fig. 1). This antibody pattern is consistent with prior localization of Kv4.2 to the transverse tubule system (Takeuchi *et al.* 2000). The signal is shown to be specific for MiRP3 and Kv4.2 because antibodies to separate epitopes of MiRP3 and Kv4.2 showed a similar staining pattern (N-14 and AB5360, respectively; not shown) and peptide block of the

primary antibodies eliminated T-tubule staining (Fig. 1*E* and *F*).

MiRP3 modulates Kv4.2 activity

Given the complexity of native cardiac cells, the functional effect of MiRP3 on Kv4.2 was assessed by studies of subunits expressed in tsA201 cells (Fig. 2 and Table 1), an approach previously used by others to study the properties of Kv4.2 with accessory subunits (Amarillo *et al.* 2008). Whole-cell currents reveal MiRP3 to slow activation and inactivation of Kv4.2 and to speed and enhance recovery from inactivation.

Figure 2*A* shows representative macroscopic Kv4.2 currents in the absence and presence of MiRP3. Current activation in response to a family of depolarizing pulses is slowed by MiRP3 leading to prolongation of the time required to reach peak current magnitude (approximately doubled at +40 mV). MiRP3 also produces a depolarizing shift of ∼+20 mV in the conductance–voltage relationship (Table 1).

MiRP3 slows Kv4.2 inactivation

The inactivating component of the outward current at +40 mV is well fitted with a dual-exponential decay function and both the fast and slow time constants are nearly doubled without affecting the weighting of the fast *versus* slow decays. Consistent with effects of MiRP3 on activation and inactivation kinetics, the steady-state inactivation of Kv4.2 is shifted by ∼10 mV (Fig. 2*B*).

Further, MiRP3 speeds recovery from inactivation ∼30% and induces peak currents that exceed baseline. Figure 2*C* shows a superimposed time series of Kv4.2 current traces for pulse pairs separated by up to 3 s at −100 mV. This overshoot phenomenon has been described for native I_{to} in human ventricular myocytes (Wettwer *et al.* 1994) and observed upon expression of MiRP1 with Kv4.2 in tissue-culture cells (Zhang *et al.* 2001).

MiRP3 alters the modulatory effects of KChIP2 on Kv4.2

The effects of KChIP2 on Kv4.2 have been described previously in detail (An *et al.* 2000; Kuo *et al.* 2001; Shibata *et al.* 2003). Kv4.2 and KChIP2 were co-expressed in the absence and presence of MiRP3. Since KChIP2 increases Kv4.2 currents so dramatically, the concentration of Kv4.2 cDNA was reduced in these experiments to prevent current saturation. Figure 3 and Table 1 show that
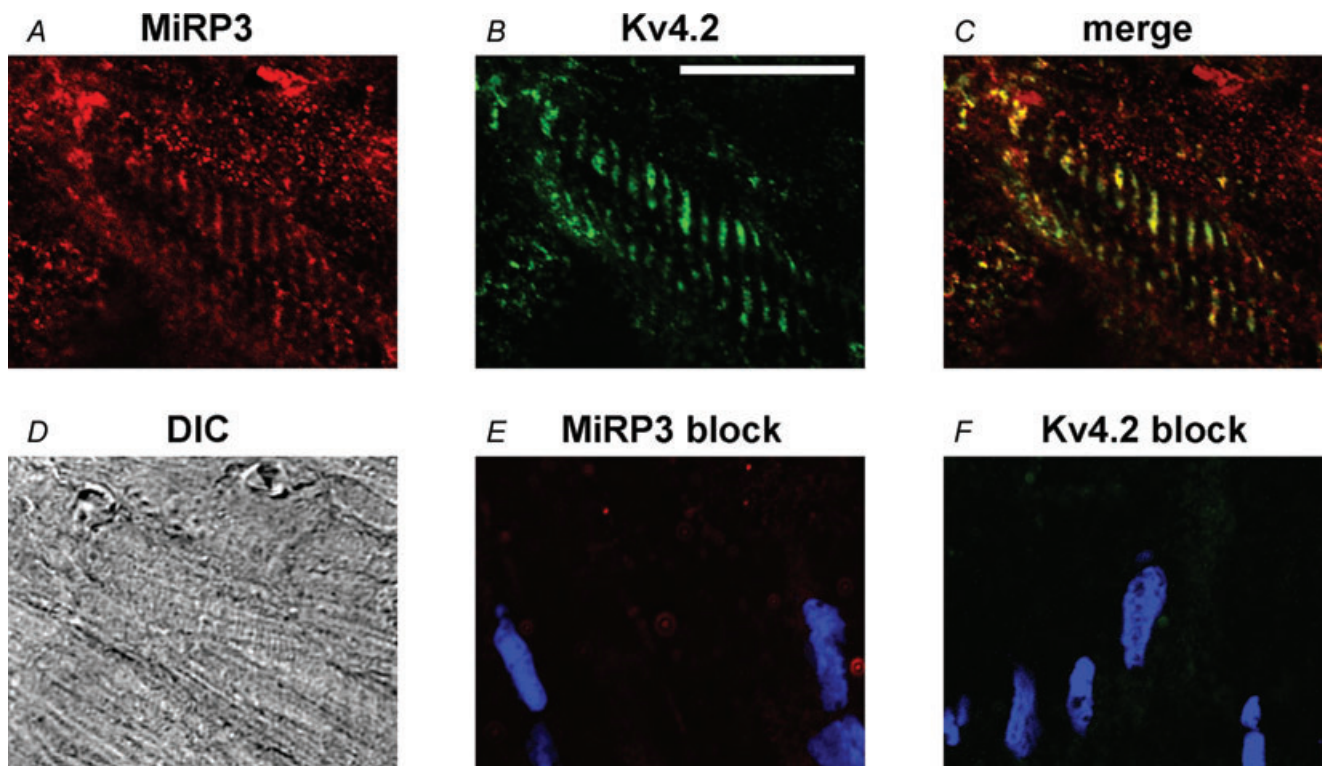

Figure 1. Spatial co-localization of MiRP3 and Kv4.2 within rat heart
Confocal images of rat left ventricle probed with antibodies to MiRP3 (*A*) and Kv4 (*B*). The T tubules appear yellow in the merged image (*C*). A differential interference contrast image (DIC, *D*) is provided for reference. Images *E* and *F* show similarly obtained confocal images when antibodies to MiRP3 and Kv4.2, respectively, were preincubated with blocking peptide; the blue colour reflects DAPI staining of nuclei. The white scale bar in *B* represents 20 μm.

Table 1. Effect of MiRP3 expression on the biophysical properties of Kv4.2 or Kv4.2/KChIP2 in tsA201 cells

	Without KChIP2 ($n = 10$–13)			With KChIP ($n = 16$–21)		
	Control	+MiRP3	P	Control	+MiRP3	P
Peak current density at +40 mV (pA pF^{-1})	660 ± 110	590 ± 90	0.65	1190 ± 220	890 ± 110	0.24
Time to peak (ms)	2.8 ± 0.2	5.8 ± 0.6	*	3.1 ± 0.1	4.1 ± 0.3	*
Inactivation τ_f (ms)	14.2 ± 0.7	26.6 ± 1.9	*	47.9 ± 1.7	50.0 ± 2.9	0.56
Inactivation τ_s (ms)	93.3 ± 7.7	146.7 ± 17	*	n/a	n/a	—
Weight of τ_f ((A_f /(A_f+A_s))*100) (%)	80.8 ± 1.9	78.0 ± 3.7	0.46	n/a	n/a	—
Non-inactivated residual at 500 ms (%)	7.6 ± 0.6	10.4 ± 1.3	0.04	4.8 ± 0.7	6.7 ± 0.9	0.11
Half-max voltage of activation ($V_{1/2\text{-act}}$; ms)	−22.7 ± 1.4	−3.3 ± 2.5	*	−17.2 ± 0.6	−13.6 ± 1.1	*
Boltzmann width for $V_{1/2\text{-act}}$ (mV)	9.3 ± 0.3	14.2 ± 0.4	*	8.6 ± 0.2	9.7 ± 0.3	*
Steady-state $V_{1/2\text{-inact}}$ (mV)	−66.9 ± 1.2	−55.2 ± 1.9	*	−53.4 ± 0.7	−53.0 ± 1.1	0.74
Boltzmann width for $V_{1/2\text{-inact}}$ (mV)	5.0 ± 1.2	6.1 ± 0.4	0.02	4.2 ± 0.2	5.4 ± 0.5	0.14
τ recovery from inactivation (ms)	74.5 ± 4.9	57.8 ± 5.1	0.047	21.8 ± 0.8	25.0 ± 2.0	0.14
Recovery overshoot (%)	0.0 ± 0.6	12.2 ± 2.2	*	2.8 ± 0.3	1.9 ± 0.4	0.08

Values shown are for mean ± S.E.M. The P values are from two-tailed Student's t test for equal variance, comparing the absence *versus* presence of MiRP3. The * indicates $P < 0.01$.

co-expression of MiRP3 and KChIP2 modifies the effects of both accessory subunits. Thus, MiRP3 alone shifts activation $V_{1/2}$ ~20 mV, KChIP2 alone shifts activation $V_{1/2}$ ~5 mV and together the shift is an intermediate ~10 mV. MiRP3 alone speeds time to peak ~100%, KChIP2 alone speeds activation ~10% and together the shift is also intermediate, ~50% faster. MiRP3 alone slows both fast and slow components of inactivation ~100%, KChIP2 alone slows inactivation ~150% and such that it proceeds in a monoexponential manner; with both accessory subunits the channel inactivates as if KChIP2 is acting alone. MiRP3 on its own and KChIP2 alone shift the steady-state inactivation $V_{1/2}$ ~15 mV and together the change is ~15 mV, like either subunit on its own. MiRP3 alone speeds recovery from inactivation ~30% and produces overshoot; KChIP2 alone speeds recovery from inactivation ~350% and shows no significant overshoot. With both accessory subunits, channels recover rapidly without overshoot, as they do with KChIP2 alone.

MiRP3 and Kv4.2 form detergent-stable associations

Biochemical association between MiRP3 and Kv4.2 was confirmed by expressing the two proteins in COS-7 cells using an epitope-tagged variant of human Kv4.2 (Kv4.2–1d4), a strategy we have used previously to demonstrate co-assembly of Kv4.2 and KChIP2 (Kim *et al.* 2004*a,b*). Proteins were purified after detergent lysis of cells via monoclonal antibodies specific to the tag. Figure 4 shows MiRP3 and Kv4.2 are purified together indicating they form detergent-stable complexes. Recovery is shown to be specific because MiRP3 is not captured when the channel has no tag or when MiRP3 or Kv4.2–1d4 are expressed alone. Coassembly of Kv4.2 and MiRP3 within the cells rather than secondarily after solubilization is demonstrated by inability to co-purify MiRP3 after mixing

lysates of separate cells expressing Kv4.2–1d4 or MiRP3. Multiple bands for MiRP3 reflect glycosylation of the protein (Levy *et al.* 2008).

MiRP3 interacts with KChIP2 via Kv4.2

Lysates from tsA201 cells expressing Kv4.2–1d4, KChIP2 and MiRP3 were studied next (Fig. 5). Immuno-purification via MiRP3 allows recovery of KChIP2 and Kv4.2 (Fig. 5*A*, lane IPb). In contrast, KChIP2 is not purified via MiRP3 when Kv4.2 is absent (Fig. 5*A*, lane IPc); this demonstrates that the formation of a three-way complex requires Kv4.2. Similar results were achieved with an antibody to residues 136–150 of MiRP3 (not shown). Immunoprecipitation of KChIP2 also allows for recovery of MiRP3 and Kv4.2 (Fig. 5*B*, lane IPc). In this case, however, a signal for the immature unglycosylated form of MiRP3 is also seen in the absence of Kv4.2 (Fig. 5*B*, lane IPb); this suggests that the two accessory subunits can interact in the absence of Kv4.2 in a location away from the plasma membrane. This association was not observed with either MiRP3 antibody (Fig. 5*A*, lane IPc), apparently because those antibodies purified the glycoslyated, membrane form of the protein, indicating either that the two accessory subunits do not interact when MiRP3 is mature or at this location.

MiRP3 interacts with filamin, but does not depend on filamin to associate with Kv4.2

The ubiquitous cytoskeletal protein filamin A has been shown to bind Kv4.2 and may be involved in chaperoning the channel complex to various subcellular locations (Petrecca *et al.* 2000). Therefore, a role for filamin A in assembly of Kv4.2–MiRP3 complexes was evaluated. First, an association of MiRP3 and filamin A was suggested by a

yeast two-hybrid screen; the screen also yielded sequences for obscurin-like protein 1 (OBSL1; NM_015311) (Geisler *et al.* 2007) and translin-associated factor X (TSNAX; NM_005999) (Schroer *et al.* 2007) that were not investigated any further. Next, association of MiRP3 and filamin A was confirmed by co-immunoprecipitation in COS-7 cells (Fig. 6*A*, lane IPc). It was demonstrated that filamin A is not required for stable association of Kv4.2 and MiRP3 by expression of the two subunits in a melanoma cell line that lacks filamin A (M2) and in a control M2 line stably transfected with filamin A (A7) (Cunningham *et al.* 1992), with successful co-immunopurification via Kv4.2–1d4 in both cases (Fig. 6*B*).

Discussion

MinK-related peptides are accessory subunits that modulate many properties of voltage-gated potassium channels. They are widely expressed (McCrossan & Abbott, 2004) and their promiscuous interactions with ion channels (Abbott & Goldstein, 2002) suggest their varied tissue-specific partners have yet to be identified. In the myocardium, all five genes of the KCNE family are transcribed (Lundquist *et al.* 2005, 2006; Radicke *et al.* 2006), although the functions of the family members remain to be elucidated. The level of mRNA for *KCNE4* (which encodes MiRP3) in human ventricle is higher
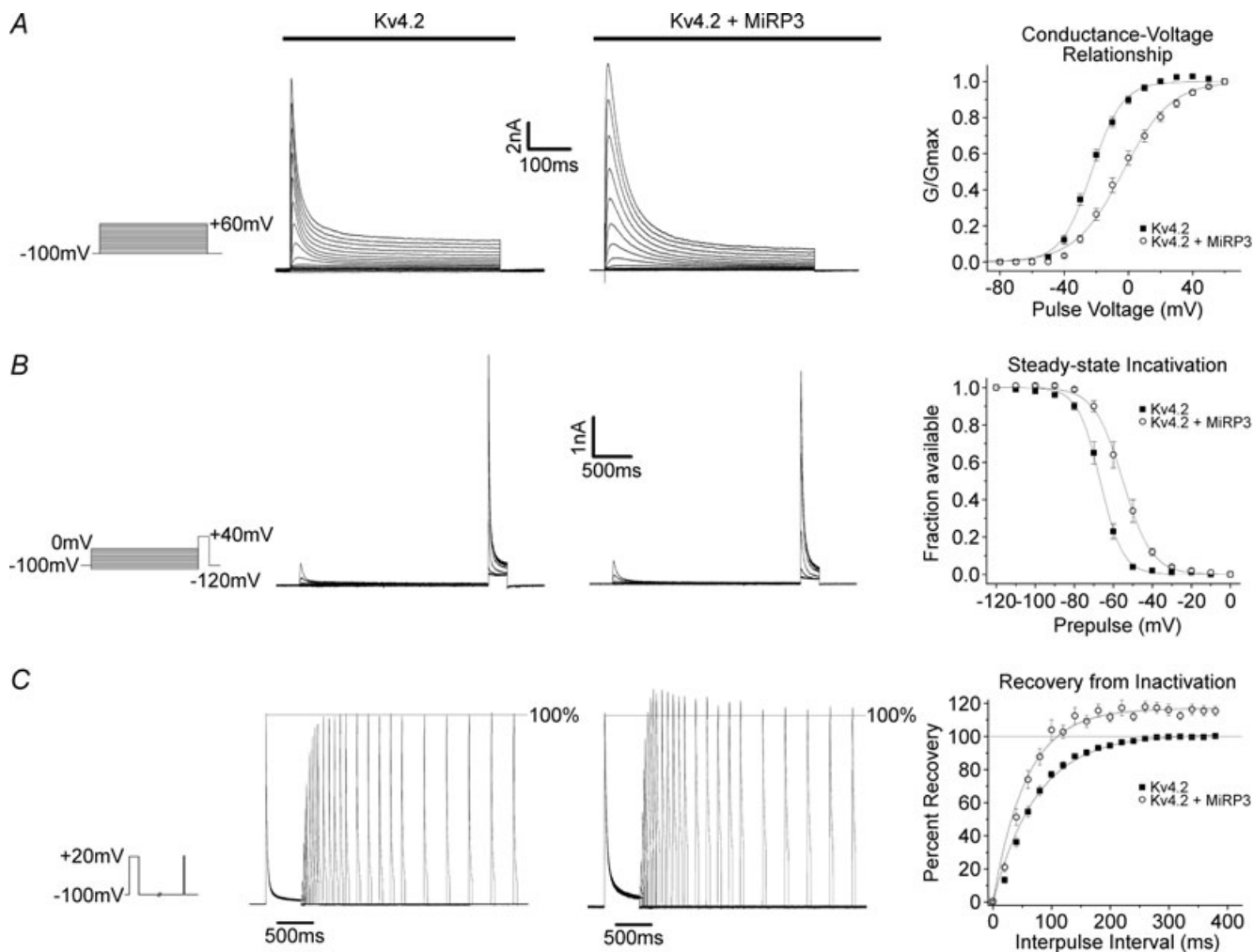

Figure 2. MiRP3 modulates Kv4.2 activity
A, representative macroscopic whole-cell recordings made from tsA201 cells transfected with hKv4.2 ± hMiRP3, in response to a family of depolarizing pulses. Panel to the right shows Boltzmann fits to mean conductance values (± S.E.M., *n* = 13 and 10, respectively). *B*, sample traces for +40 mV pulses delivered after a 2.5 s prepulse. Graph shows Boltzmann fits to residual currents (relative to the first +40 mV pulse) as a function of the prepulse. *C*, representative currents from a two-pulse protocol with a variable interpulse interval at −100 mV. Currents were scaled so that the peak of the first pulse was 100%. Single-exponential fits to recovery from the two families shown yielded τ values of 80.5 ms and 62.3 ms in the absence and presence of MiRP3, with plateaus overshooting the first paired pulse by 0.1% and 10.9%, respectively. Fits to the mean per cent of recovery (± S.E.M.) are plotted as a function of the interpulse interval.
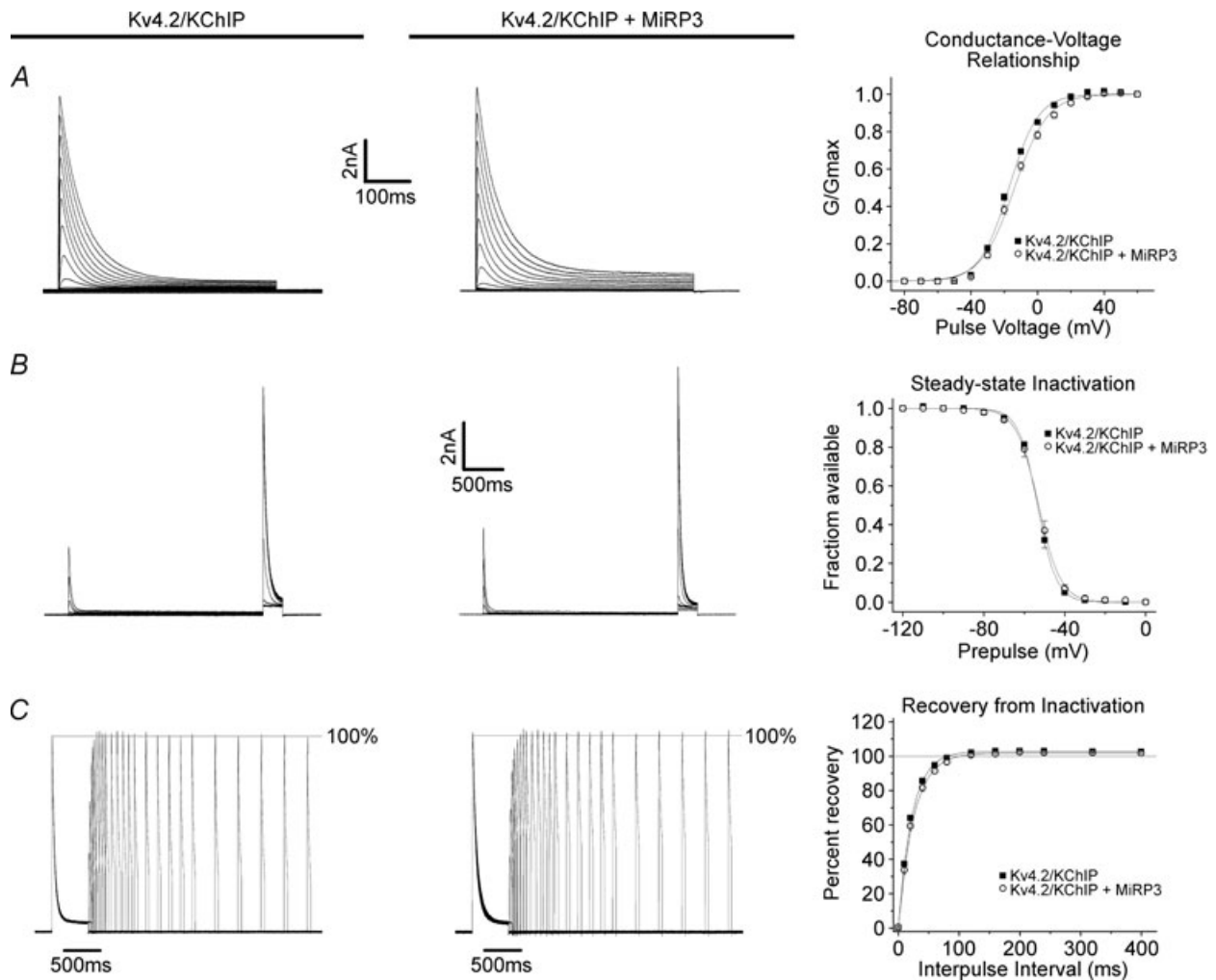
Figure 3. KChIP2 interferes with MiRP3 modulation of Kv4.2 kinetics
A–C, representative traces and fits to data (*n* = 16–21) obtained as described for Fig. 2, from tsA201 cells transfected with hKChIP2.1/hKv4.2 cDNA (in pIRES) and either empty vector or hMiRP3.

than other members of the family (Lundquist *et al.* 2006; Radicke *et al.* 2006) and found to be increased in human heart failure in one study (Lundquist *et al.* 2005). Here, we provide evidence suggesting a role for MiRP3 in formation and operation of native cardiac I_{to} via association with Kv4.2 and KChIP2.

Supporting the participation of MiRP3 in the cardiac I_{to} current, MiRP3 and Kv4.2 were co-localized to the T-tubules of murine ventricular myocytes. Further, co-expression of the three proteins in tissue culture cells leads to formation of detergent-stable ternary complexes that can be purified with antibodies towards either MiRP3 or KChIP2. It was additionally noted that the cytoskeletal scaffolding protein filamin A can assemble with MiRP3 or Kv4.2 independently and is not required for their stable assembly.

Figure 4. Stable biochemical interaction between MiRP3 and Kv4.2
COS-7 cells transfected with MiRP3 (a), MiRP3 and Kv4.2 (b), MiRP3 and Kv4.2–1d4 (c), or Kv4.2–1d4 alone (d), were subjected to lysis and immunopurification (IP) with anti-1d4 antibodies. An additional treatment group (e) consisted of lysate from cells expressing MiRP3 mixed with lysate from cells expressing Kv4.2–1d4, at 4°C for 16 h prior to immunopurification. Blots were probed with antibodies to Kv4.2 (70 kDa) and MiRP3 (21–25 kDa).
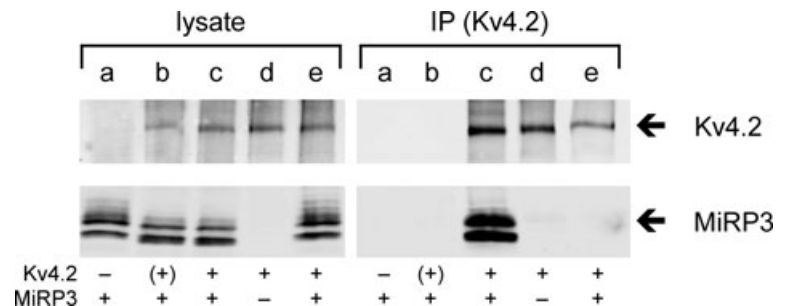
Studied in tsA201 cells in the absence of KChIP2, MiRP3 alters Kv4.2 channel function, slowing activation and inactivation, shifting $V_{1/2}$ for activation and inactivation, speeding recovery from inactivation, and producing overshoot. MiRP3 also alters the biophysical effects of KChIP2 on channels formed with Kv4.2. Like co-purification, these biophysical effects of MiRP3 indicate we are studying a novel population of channels that contains all three subunits. Thus, study of a mixture of Kv4.2–KChIP2 and Kv4.2–MiRP3 channels would neither eliminate MiRP3-induced biexponential inactivation kinetics nor overshoot in recovery from inactivation (as if only Kv4.2–KChIP2 channels were studied) while retaining MiRP3-induced slowing of time to peak and shift in $V_{1/2}$ for activation (Table 1). How these parameters may be altered in their different, native cardiac milieu remains to be clarified.

The spatial and temporal plasticity of I_{to} across the myocardial wall, the variety of accessory proteins implicated in its operation, and the variation in partnerships in different species and pathophysiological conditions (Patel & Campbell, 2005; Niwa & Nerbonne, 2010) make it important to resolve the diverse roles of accessory subunits in heart function; these same factors make elucidation of the specific roles of each subunit a challenge. Some aspects of KCNE-family proteins function in the heart have been elucidated. Evidence for assembly of MinK and KCNQ1 to form cardiac I_{Ks} channels includes comparison of native currents and those studied with cloned subunits, clinical consequences of mutations in *KCNQ1* and *KCNE1* genes, and the achievement of their co-purification from horse cardiac tissue (Finley *et al.* 2002). MinK has also been implicated in the operation of I_{Kr} channels (formed by hERG subunits) (McDonald *et al.* 1997).

MiRP1 has been linked to the operation of I_{Kr} channels with mutations and polymorphisms associated with congenital and acquired long QT syndrome (Abbott *et al.* 1999; Sesti *et al.* 2000; Park *et al.* 2003), an association demonstrated directly by co-isolation of MiRP1 and ERG from dog heart (Jiang *et al.* 2004). In tissue culture cells, MiRP1 has been implicated in modulation of the Kv4.2/Kv4.3 (Zhang *et al.* 2001) subunits producing I_{to} and the hyperpolarization-activated cation channel subunits that underlie I_f (Yu *et al.* 2001; Proenza *et al.* 2002; Decher *et al.* 2003). Recently, targeted deletion of MiRP1 in mice (which do not express abundant ERG in adulthood) was found to cause moderate changes in I_{to} and $I_{K,slow1}$, effects attributed to loss of impact on murine Kv4.2 and Kv1.5 subunits, respectively, and supported by co-immunoprecipitation of MiRP1–Kv4.2 and MiRP1–Kv1.5 complexes from normal mouse heart (Roepke *et al.* 2008).
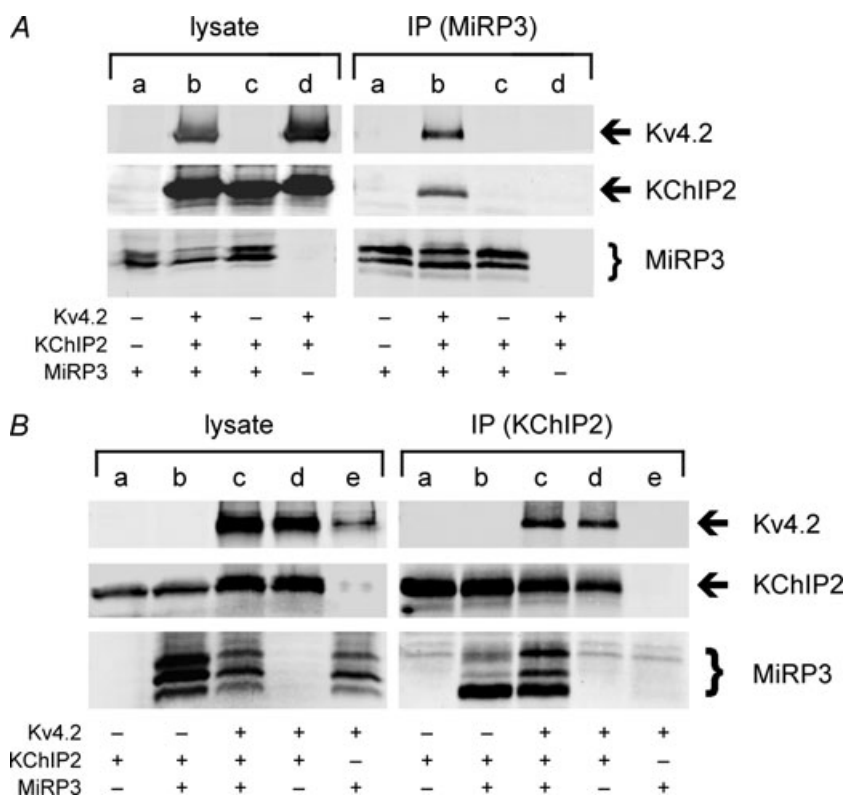

Figure 5. Ternary interactions between MiRP3, Kv4.2 and KChIP2

A, MiRP3 was immunopurified from lysates of tsA201 cells transfected with MiRP3 (a), MiRP3, Kv4.2 and KChIP2 (b), MiRP3 and KChIP2 (c), or Kv4.2 and KChIP2 (d). *B*, KChIP2 was immunoprecipitated from lysates of tsA201 cells transfected with KChIP2 (a), MiRP3 and KChIP2 (b), MiRP3, Kv4.2 and KChIP2 (c), Kv4.2 and KChIP2 (d), or MiRP3 and Kv4.2 (e). Images of blots span roughly 65–80 kDa for Kv4.2, 24–31 kDa for KChIP, and 20–28 kDa for MiRP3. Faint bands at 25–26 kDa in all five lanes of the IP blotted for MiRP3 are presumed to be crossreactivity of secondary antibodies to immunoprecipitated KChIP2 antibody.

MiRP2 also appears to participate in the modulation of cardiac currents. Genetic studies have shown that phenotype-positive members of a family with Brugada syndrome carried an R99H missense mutation in *KCNE3* and this was speculated (based on *in vitro* studies with Kv4.2) to impact on I_{to} (Delpón *et al.* 2008). This same mutation of MiRP2 has been implicated in long QT syndrome because *in vitro* studies showed it could reduce currents passed by KCNQ1 (Ohno *et al.* 2009). Finally, MiRP4 may also be involved in modulating cardiac ion channels, as it too is expressed in heart and can inhibit KCNQ1 and Kv4 channels *in vitro* (Angelo *et al.* 2002; Bendahhou *et al.* 2005; Lundquist *et al.* 2005; Radicke *et al.* 2006).

MiRP3 has previously been suggested to contribute to the operation of cardiac I_{Ks} and I_{to}. MiRP3 forms a ternary complex with KCNQ1 and MinK in tissue culture cells where it strongly suppresses I_{Ks} current (Lundquist *et al.* 2005; Manderfield & George, 2008). The high level of KCNE4 transcript in the heart seems

at odds with measurement of significant I_{Ks} currents. However, modulation of I_{Ks} will depend on rates of synthesis of MinK and MiRP3 and other cell-specific factors that alter preferential assembly with KCNQ1 (Morin & Kobertz, 2007) as found for MiRP2 with Kv2.1 or Kv3.1 in different cells in the nervous system (McCrossan *et al.* 2003). Similar, cell-specific effects are expected for MiRP3 and KChIP2 with Kv4.2. Radicke *et al.* (2006) have previously implicated MiRP3 in operation of human I_{to} by showing high levels of *KCNE4* transcript in the heart that change with cardiomyopathy and functional modulation of channels formed by Kv4.3 and KChIP2. Perhaps due to isoform differences, their findings vary from ours in that they observe MiRP3 to speed time to peak current, to speed inactivation, and to enhance recovery from inactivation of Kv4.3 with KChIP2; whereas we observe MiRP3 to slow time to peak and shift activation $V_{1/2}$ ~5 mV, while the channels inactivate and recover from inactivation as if KChIP2 is acting alone on Kv4.2. These differences suggest specific roles for MiRP3 in cardiac repolarization
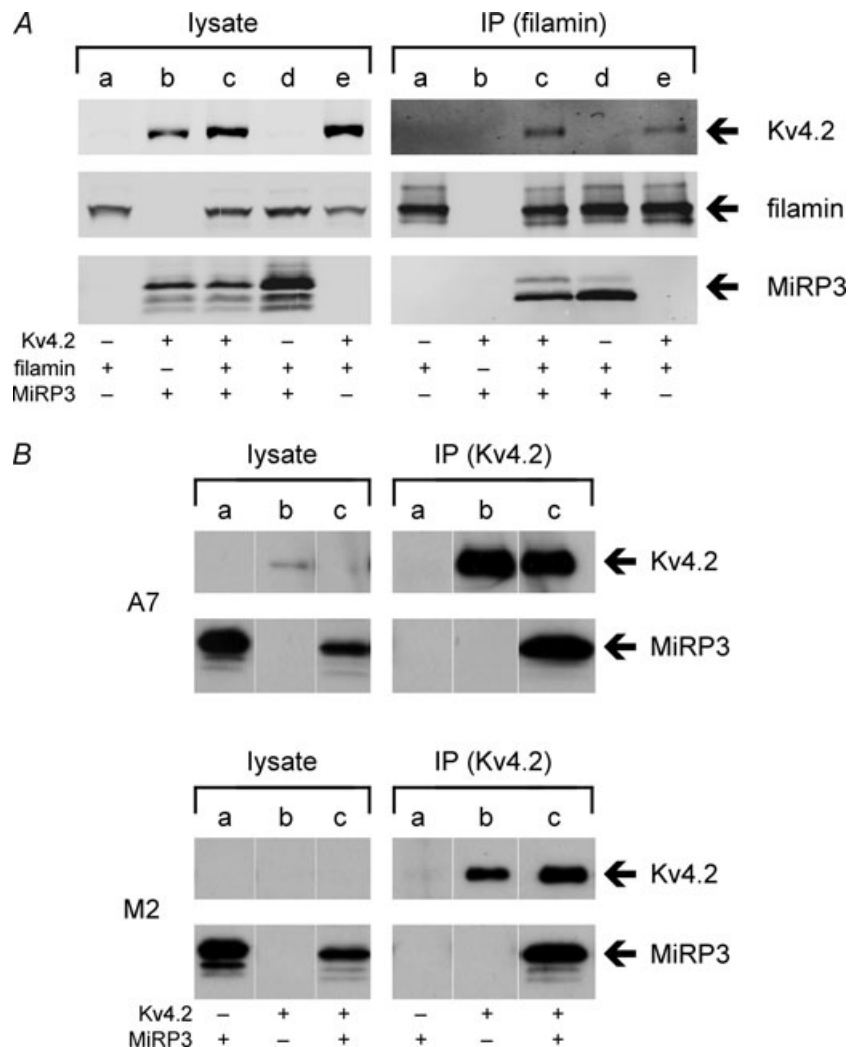

Figure 6. Interactions between filamin A, MiRP3 and Kv4.2

A, COS-7 cells were transfected with fil–1d4 (a), MiRP3 and Kv4.2 (b), MiRP3, fil–1d4 and Kv4.2 (c), MiRP3 and fil–1d4 (d), or fil–1d4 and Kv4.2 (e). Cells were lysed and immunopurified (IP) with anti-1d4 antibodies. Note that low quantities of co-purified Kv4.2 required high-sensitivity scanning to detect signal. *B*, co-purification of MiRP3 with Kv4.2 in filamin-replete (A7) and filamin-deplete (M2) cells. Western blots show lysates and epitope-purified fractions from cells transfected with MiRP3 (a), Kv4.2–1d4 (b), or MiRP3 and Kv4.2–1d4 (c).

in cells that primarily employ Kv4.3, Kv4.2 or heteromeric Kv4.2/Kv4.3 channels (Guo *et al.* 2002; Patel & Campbell, 2005).

Native-tissue co-immunoprecipitation is the most convincing manner to establish the presence of subunit partners as accomplished for MinK and KCNQ1 in equine heart (Finley *et al.* 2002), MiRP1 and ERG in dog heart (Jiang *et al.* 2004) and MiRP1 with Kv4.2 and Kv1.5 in mouse heart (Roepke *et al.* 2008); this has not yet been achieved with MiRP3. Given the dynamic expression of the I_{to}-related proteins across the wall of the myocardium, adequate understanding of all these complexes may require novel techniques to evaluate complexes from single cells.

How might MiRP3 influence I_{to} currents? *KCNE4* is expressed uniformly and robustly across the ventricular wall while Kv4.2 or KChIP2 vary in a species-dependent manner (Bendahhou *et al.* 2005; Radicke *et al.* 2006). As MiRP3 modifies operation of Kv4.2 differently when it is assembled with KChIP2, the effects will vary in spatial fashion with KChIP2. In channels with KChIP2, MiRP3 should have only a modest inhibitory effect on I_{to} due to prolongation of the time to peak current and the depolarizing shift of the $V_{1/2\text{-act}}$. In the absence of KChIP2 one expects a different picture, notable for marked reduction in I_{to} due to loss of KChIP2-mediated facilitation of Kv4.2 channel surface expression (Shibata *et al.* 2003) and altered current morphology resulting from MiRP3-induced slowing of activation, inactivation of currents with biexponential kinetics and enhanced recovery from inactivation. Thus, endocardial myocytes with Kv4.2 and MiRP3 and little or no KChIP2 (Rosati *et al.* 2001; Schultz *et al.* 2005) are those expected to demonstrate these characteristics Similarly, KChIP2 transcript is reduced in human cardiomyopathic heart while mRNA levels for the genes encoding Kv4 and MiRP3 appear to be relatively stable (Radicke *et al.* 2006). Under these circumstances, MiRP3 may again serve to further reduce and modify the attributes of potassium flux beyond those that accrue from the absence of KChIP2, such as, maintaining the slow inactivation kinetics of I_{to} that persist in congestive heart failure (Tomaselli *et al.* 1994; Wettwer *et al.* 1994).

References

Abbott GW & Goldstein SA (1998). A superfamily of small potassium channel subunits: form and function of the MinK-related peptides (MiRPs). *Q Rev Biophys* **31**, 357–398.

Abbott GW & Goldstein SA (2002). Disease-associated mutations in *KCNE* potassium channel subunits (MiRPs) reveal promiscuous disruption of multiple currents and conservation of mechanism. *FASEB J* **16**, 390–400.

Abbott GW, Sesti F, Splawski I, Buck ME, Lehmann MH, Timothy KW, Keating MT & Goldstein SA (1999). MiRP1 forms I_{Kr} potassium channels with HERG and is associated with cardiac arrhythmia. *Cell* **97**, 175–187.

Amarillo Y, De Santiago-Castillo JA, Dougherty K, Maffie J, Kwon E, Covarrubias M & Rudy B (2008). Ternary Kv4.2 channels recapitulate voltage-dependent inactivation kinetics of A-type K^+ channels in cerebellar granule neurons. *J Physiol* **586**, 2093–2106.

An WF, Bowlby MR, Betty M, Cao J, Ling HP, Mendoza G, Hinson JW, Mattsson KI, Strassle BW, Trimmer JS & Rhodes KJ (2000). Modulation of A-type potassium channels by a family of calcium sensors. *Nature* **403**, 553–556.

Angelo K, Jespersen T, Grunnet M, Nielsen MS, Klaerke DA & Olesen SP (2002). KCNE5 induces time- and voltage-dependent modulation of the KCNQ1 current. *Biophys J* **83**, 1997–2006.

Barhanin J, Lesage F, Guillemare E, Fink M, Lazdunski M & Romey G (1996). KvLQT1 and IsK (minK) proteins associate to form the I_{Ks} cardiac potassium current. *Nature* **384**, 78–80.

Bendahhou S, Marionneau C, Haurogne K, Larroque MM, Derand R, Szuts V, Escande D, Demolombe S & Barhanin J (2005). *In vitro* molecular interactions and distribution of KCNE family with KCNQ1 in the human heart. *Cardiovasc Res* **67**, 529–538.

Bianchi L, Kwok SM, Driscoll M & Sesti F (2003). A potassium channel-MiRP complex controls neurosensory function in *Caenorhabditis elegans*. *J Biol Chem* **278**, 12415–12424.

Bockenhauer D, Zilberberg N & Goldstein SA (2001). KCNK2: reversible conversion of a hippocampal potassium leak into a voltage-dependent channel. *Nat Neurosci* **4**, 486–491.

Clay JR (2000). Determining K^+ channel activation curves from K^+ channel currents. *Eur Biophys J* **29**, 555–557.

Cunningham CC, Gorlin JB, Kwiatkowski DJ, Hartwig JH, Janmey PA, Byers HR & Stossel TP (1992). Actin-binding protein requirement for cortical stability and efficient locomotion. *Science* **255**, 325–327.

Decher N, Bundis F, Vajna R & Steinmeyer K (2003). KCNE2 modulates current amplitudes and activation kinetics of HCN4: influence of KCNE family members on HCN4 currents. *Pflugers Arch* **446**, 633–640.

Delpón E, Cordeiro JM, Núñez L, Thomsen PE, Guerchicoff A, Pollevick GD, Wu Y, Kanters JK, Larsen CT, Burashnikov E, Christiansen M & Antzelevitch C (2008). Functional effects of *KCNE3* mutation and its role in the development of Brugada syndrome. *Circ Arrhythm Electrophysiol* **1**, 209–218.

Finley MR, Li Y, Hua F, Lillich J, Mitchell KE, Ganta S, Gilmour RF Jr & Freeman LC (2002). Expression and coassociation of ERG1, KCNQ1, and KCNE1 potassium channel proteins in horse heart. *Am J Physiol Heart Circ Physiol* **283**, H126–H138.

Geisler SB, Robinson D, Hauringa M, Raeker MO, Borisov AB, Westfall MV & Russell MW (2007). Obscurin-like 1, OBSL1, is a novel cytoskeletal protein related to obscurin. *Genomics* **89**, 521–531.

Grunnet M, Jespersen T, Rasmussen HB, Ljungstrom T, Jorgensen NK, Olesen SP & Klaerke DA (2002). KCNE4 is an inhibitory subunit to the KCNQ1 channel. *J Physiol* **542**, 119–130.

Guo W, Jung WE, Marionneau C, Aimond F, Xu H, Yamada KA, Schwarz TL, Demolombe S & Nerbonne JM (2005). Targeted deletion of Kv4.2 eliminates $I_{to,f}$ and results in electrical and molecular remodelling, with no evidence of ventricular hypertrophy or myocardial dysfunction. *Circ Res* **97**, 1342–1350.

Guo W, Li H, Aimond F, Johns DC, Rhodes KJ, Trimmer JS & Nerbonne JM (2002). Role of heteromultimers in the generation of myocardial transient outward K$^+$ currents. *Circ Res* **90**, 586–593.

Guo W, Xu H, London B & Nerbonne JM (1999). Molecular basis of transient outward K$^+$ current diversity in mouse ventricular myocytes. *J Physiol* **521**, 587–599.

Jiang M, Zhang M, Tang DG, Clemo HF, Liu J, Holwitt D, Kasirajan V, Pond AL, Wettwer E & Tseng GN (2004). KCNE2 protein is expressed in ventricles of different species, and changes in its expression contribute to electrical remodelling in diseased hearts. *Circulation* **109**, 1783–1788.

Kim LA, Furst J, Butler MH, Xu S, Grigorieff N & Goldstein SA (2004*a*). I_{to} channels are octomeric complexes with four subunits of each Kv4.2 and K$^+$ channel-interacting protein 2. *J Biol Chem* **279**, 5549–5554.

Kim LA, Furst J, Gutierrez D, Butler MH, Xu S, Goldstein SA & Grigorieff N (2004*b*). Three-dimensional structure of I_{to}: Kv4.2-KChIP2 ion channels by electron microscopy at 21 Angstrom resolution. *Neuron* **41**, 513–519.

Kuo HC, Cheng CF, Clark RB, Lin JJ, Lin JL, Hoshijima M, Nguyen-Tran VT, Gu Y, Ikeda Y, Chu PH, Ross J, Giles WR & Chien KR (2001). A defect in the Kv channel-interacting protein 2 (KChIP2) gene leads to a complete loss of I_{to} and confers susceptibility to ventricular tachycardia. *Cell* **107**, 801–813.

Levy DI, Wanderling S, Biemesderfer D & Goldstein SA (2008). MiRP3 acts as an accessory subunit with the BK potassium channel. *Am J Physiol Renal Physiol* **295**, F380–F387.

Lundquist AL, Manderfield LJ, Vanoye CG, Rogers CS, Donahue BS, Chang PA, Drinkwater DC, Murray KT & George AL Jr (2005). Expression of multiple KCNE genes in human heart may enable variable modulation of I_{Ks}. *J Mol Cell Cardiol* **38**, 277–287.

Lundquist AL, Turner CL, Ballester LY & George AL Jr (2006). Expression and transcriptional control of human KCNE genes. *Genomics* **87**, 119–128.

McCrossan ZA & Abbott GW (2004). The MinK-related peptides. *Neuropharmacology* **47**, 787–821.

McCrossan ZA, Lewis A, Panaghie G, Jordan PN, Christini DJ, Lerner DJ & Abbott GW (2003). MinK-related peptide 2 modulates Kv2.1 and Kv3.1 potassium channels in mammalian brain. *J Neurosci* **23**, 8077–8091.

McDonald TV, Yu Z, Ming Z, Palma E, Meyers MB, Wang KW, Goldstein SA & Fishman GI (1997). A minK-HERG complex regulates the cardiac potassium current I_{Kr}. *Nature* **388**, 289–292.

Manderfield LJ, Daniels MA, Vanoye CG & George AL Jr (2009). KCNE4 domains required for inhibition of KCNQ1. *J Physiol* **587**, 303–314.

Manderfield LJ & George AL Jr (2008). KCNE4 can co-associate with the I_{Ks} (KCNQ1-KCNE1) channel complex. *FEBS J* **275**, 1336–1349.

Morin TJ & Kobertz WR (2007). A derivatized scorpion toxin reveals the functional output of heteromeric KCNQ1-KCNE K$^+$ channel complexes. *ACS Chem Biol* **2**, 469–473.

Niwa N & Nerbonne JM (2010). Molecular determinants of cardiac transient outward potassium current I_{to} expression and regulation. *J Mol Cell Cardiol* **48**, 12–25.

Niwa N, Wang W, Sha Q, Marionneau C & Nerbonne JM (2008). Kv4.3 is not required for the generation of functional $I_{to,f}$ channels in adult mouse ventricles. *J Mol Cell Cardiol* **44**, 95–104.

Ohno S, Toyoda F, Zankov DP, Yoshida H, Makiyama T, Tsuji K, Honda T, Obayashi K, Ueyama H, Shimizu W, Miyamoto Y, Kamakura S, Matsuura H, Kita T & Horie M (2009). Novel KCNE3 mutation reduces repolarizing potassium current and associated with long QT syndrome. *Hum Mutat* **30**, 557–563.

Park KH, Kwok SM, Sharon C, Baerga R & Sesti F (2003). N-Glycosylation-dependent block is a novel mechanism for drug-induced cardiac arrhythmia. *FASEB J* **17**, 2308–2309.

Patel SP & Campbell DL (2005). Transient outward potassium current, 'I_{to}', phenotypes in the mammalian left ventricle: underlying molecular, cellular and biophysical mechanisms. *J Physiol* **569**, 7–39.

Patel SP, Campbell DL, Morales MJ & Strauss HC (2002). Heterogeneous expression of KChIP2 isoforms in the ferret heart. *J Physiol* **539**, 649–656.

Petrecca K, Miller DM & Shrier A (2000). Localization and enhanced current density of the Kv4.2 potassium channel by interaction with the actin-binding protein filamin. *J Neurosci* **20**, 8736–8744.

Proenza C, Angoli D, Agranovich E, Macri V & Accili EA (2002). Pacemaker channels produce an instantaneous current. *J Biol Chem* **277**, 5101–5109.

Radicke S, Cotella D, Graf EM, Banse U, Jost N, Varro A, Tseng GN, Ravens U & Wettwer E (2006). Functional modulation of the transient outward current I_{to} by KCNE β-subunits and regional distribution in human non-failing and failing hearts. *Cardiovasc Res* **71**, 695–703.

Roepke TK, Kontogeorgis A, Ovanez C, Xu X, Young JB, Purtell K, Goldstein PA, Christini DJ, Peters NS, Akar FG, Gutstein DE, Lerner DJ & Abbott GW (2008). Targeted deletion of *kcne2* impairs ventricular repolarization *via* disruption of $I_{K,slow1}$ and $I_{to,f}$. *FASEB J* **22**, 3648–3660.

Rosati B, Pan Z, Lypen S, Wang HS, Cohen I, Dixon JE & McKinnon D (2001). Regulation of *KChIP2* potassium channel β subunit gene expression underlies the gradient of transient outward current in canine and human ventricle. *J Physiol* **533**, 119–125.

Sanguinetti MC, Curran ME, Zou A, Shen J, Spector PS, Atkinson DL & Keating MT (1996). Coassembly of KvLQT1 and minK (IsK) proteins to form cardiac I_{Ks} potassium channel. *Nature* **384**, 80–83.

Schroer U, Volk GF, Liedtke T & Thanos S (2007). Translin-associated factor-X (Trax) is a molecular switch of growth-associated protein (GAP)-43 that controls axonal regeneration. *Eur J Neurosci* **26**, 2169–2178.

Schultz JH, Janzen C, Volk T & Ehmke H (2005). Kv4.2 and KChIP2 transcription in individual cardiomyocytes from the rat left ventricular free wall. *J Mol Cell Cardiol* **39**, 269–275.

Sesti F, Abbott GW, Wei J, Murray KT, Saksena S, Schwartz PJ, Priori SG, Roden DM, George AL Jr & Goldstein SA (2000). A common polymorphism associated with antibiotic-induced cardiac arrhythmia. *Proc Natl Acad Sci U S A* **97**, 10613–10618.

Sesti F & Goldstein SA (1998). Single-channel characteristics of wild-type I_{Ks} channels and channels formed with two minK mutants that cause long QT syndrome. *J Gen Physiol* **112**, 651–663.

Shibata R, Misonou H, Campomanes CR, Anderson AE, Schrader LA, Doliveira LC, Carroll KI, Sweatt JD, Rhodes KJ & Trimmer JS (2003). A fundamental role for KChIPs in determining the molecular properties and trafficking of Kv4.2 potassium channels. *J Biol Chem* **278**, 36445–36454.

Splawski I, Tristani-Firouzi M, Lehmann MH, Sanguinetti MC & Keating MT (1997). Mutations in the h*minK* gene cause long QT syndrome and suppress I_{Ks} function. *Nat Genet* **17**, 338–340.

Takeuchi S, Takagishi Y, Yasui K, Murata Y, Toyama J & Kodama I (2000). Voltage-gated K^+ channel, Kv4.2, localizes predominantly to the transverse-axial tubular system of the rat myocyte. *J Mol Cell Cardiol* **32**, 1361–1369.

Tomaselli GF, Beuckelmann DJ, Calkins HG, Berger RD, Kessler PD, Lawrence JH, Kass D, Feldman AM & Marban E (1994). Sudden cardiac death in heart failure. The role of abnormal repolarization. *Circulation* **90**, 2534–2539.

Vanoye CG, Welch RC, Daniels MA, Manderfield LJ, Tapper AR, Sanders CR & George AL Jr (2009). Distinct subdomains of the KCNQ1 S6 segment determine channel modulation by different KCNE subunits. *J Gen Physiol* **134**, 207–217.

Wettwer E, Amos GJ, Posival H & Ravens U (1994). Transient outward current in human ventricular myocytes of subepicardial and subendocardial origin. *Circ Res* **75**, 473–482.

Yao JA, Jiang M, Fan JS, Zhou YY & Tseng GN (1999). Heterogeneous changes in K currents in rat ventricles three days after myocardial infarction. *Cardiovasc Res* **44**, 132–145.

Yu H, Wu J, Potapova I, Wymore RT, Holmes B, Zuckerman J, Pan Z, Wang H, Shi W, Robinson RB, El-Maghrabi MR, Benjamin W, Dixon J, McKinnon D, Cohen IS & Wymore R (2001). MinK-related peptide 1: A β subunit for the HCN ion channel subunit family enhances expression and speeds activation. *Circ Res* **88**, E84–E87.

Zhang M, Jiang M & Tseng GN (2001). MinK-related peptide 1 associates with Kv4.2 and modulates its gating function: potential role as β subunit of cardiac transient outward channel? *Circ Res* **88**, 1012–1019.

Acknowledgements